# Fine wavelength control in 1.3 μm Nd:YAG lasers by electro-optical crystal lens

Yanfei Lü, Jing Zhang, Huilong Liu, Jing Xia, Xihong Fu, and Anfeng Zhang

Citation: Journal of Applied Physics **115**, 073102 (2014); doi: 10.1063/1.4866093
View online: http://dx.doi.org/10.1063/1.4866093
View Table of Contents: http://scitation.aip.org/content/aip/journal/jap/115/7?ver=pdfcov
Published by the AIP Publishing



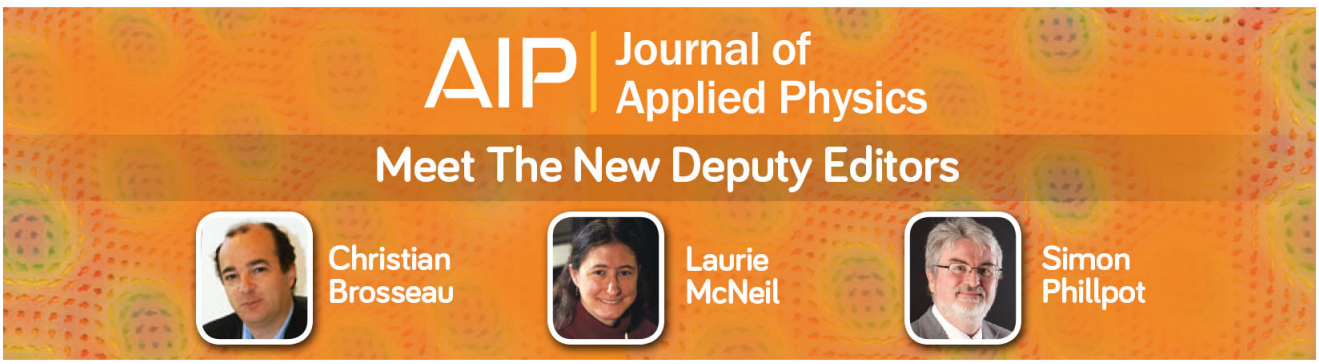

# Fine wavelength control in 1.3 μm Nd:YAG lasers by electro-optical crystal lens

Yanfei Lü,[1,a)] Jing Zhang,[1] Huilong Liu,[1] Jing Xia,[1] Xihong Fu,[2] and Anfeng Zhang[3]
[1]School of Science, Changchun University of Science and Technology, Changchun 130022, China
[2]State Key Laboratory of Luminescence and Applications, Changchun Institute of Optics, Fine Mechanics and Physics, Chinese Academy of Sciences, Changchun 130033, China
[3]Laboratory of Info-integration Technology, Xi'an Institute of Applied Optics, Xi'an 710065, China

(Received 19 November 2013; accepted 5 February 2014; published online 19 February 2014)

A diode-pumped tunable and multi-wavelength continuous-wave Nd:YAG laser based on the $^4F_{3/2}-^4I_{13/2}$ transition has been demonstrated for the first time. The combination of the glass plane positioned at the Brewster angle and the electro-optical crystal $KH_2PO_4$ (KDP) lens formed a Lyot filter in the cavity and compressed the available gain bandwidth. With an adjustable voltage applied to the KDP crystal lens, the laser wavelength could be tuned from 1333.8 to 1338.2 nm. Moreover, we can also realize cw dual-wavelength and triple-wavelength lasers with smaller wavelength separation by adjusting the free spectral range of the Lyot filter. © *2014 AIP Publishing LLC*. [http://dx.doi.org/10.1063/1.4866093]

## I. INTRODUCTION

All-solid-state 1.3–1.4 μm lasers have attracted a great deal of attentions for its applications in laser medicine, fiber communications system, non-linear frequency conversion to produce visible radiation, and so on.[1,2] The $^4F_{3/2}-^4I_{13/2}$ transition of $Nd^{3+}$-doped crystal locates in this wavelength region. The Nd:YAG crystal has been most widely used as a kind of solid-state laser medium so far. The diagram of energy levels of $Nd^{3+}$ ion in YAG crystal on the $^4F_{3/2}-^4I_{13/2}$ transition is shown in Fig. 1. The $^4F_{3/2}-^4I_{13/2}$ transitions of $Nd^{3+}$ ion are located in the 1.3–1.4 μm wavelengths region, from which there are eleven emission lines due to the split of stark energy levels. Because the stimulated emission cross sections of 1318.8, 1320, 1333.8, 1335, 1338.2, 1341, 1353.6, 1356.4, 1414, 1430.8, 1444 nm transitions are less than those of 1319 and 1338.2 nm, the laser emissions of these wavelengths cannot compete against those of 1319 and 1338.2 nm during the laser operation. In addition, the emission cross sections of the adjacent transition wavelengths are very close. For example, the stimulated emission cross sections of 1333.8 and 1335 nm are $3.0 \times 10^{-20}$ and $3.4 \times 10^{-20}$ $cm^2$, respectively.[3] Moreover, the interval of the two peaks is only 1.2 nm. Thus, it is difficult to realize the oscillation of single wavelength by suppressing the other with coatings. In order to obtain the single-wavelength output in narrow band range, an etalon is usually inserted in the cavity to select wavelength.[4–6] However, when tuning with the etalon, mechanical rotation is necessary, which lowers the adjusting accuracy and can only realize single-wavelength output. In this paper, we propose a new tunable method for narrow band range by applying an adjustable voltage to the $KH_2PO_4$ (KDP) crystal lens. We achieved a diode-pumped tunable cw Nd:YAG laser based on the $^4F_{3/2}-^4I_{13/2}$ transition, and the laser wavelength could be tuned from 1333.8 to 1338.2 nm.

Multi-wavelength laser with the smaller separation would be especially valuable as a compact and strong laser source to generate the THz emission because the frequency difference[7] between two wavelengths is about 0.7 THz. Coherent THz waves, traditionally defined in the frequency range of 0.1–3 THz, have great potential for THz imaging, sensing, and THz spectroscopy applications.[8–10] Up to now, the realized dual-wavelength lasers of the smaller wavelength separation in $Nd^{3+}$-doped crystals can be classified into two main categories. The first category is the laser operated in the same laser transition with a smaller wavelength separation and a single polarization.[11–13] The second category is the dual-wavelength lasers with orthogonal polarizations.[14–16] Very little research was carried out on the triple-wavelength lasers of the smaller wavelength separation.[17,18] In this paper, the output of cw dual-wavelength laser operating at 1333.8 and 1335 nm and triple-wavelength laser operating at 1333.8, 1335, and 1338.2 nm was realized in the Nd:YAG lasers. To the best of our knowledge, it is the first time that the multi-wavelength operation with such small separation is demonstrated.

## II. EXPERIMENT AND RESULT ANALYSIS

The experimental setup used is described in Fig. 2. The optical pumping was done by using fiber-coupled (diameter of 200 μm and numerical aperture NA = 0.22) diode lasers from Coherent Co., USA. The 809 nm emitting diode outputted 20 W of pump power with an emission bandwidth of 2.0 nm (FWHM definition). The coupling optics consists of two identical plano-convex lenses with focal lengths of 15 mm used to re-image the pump beam into the laser crystal at a ratio of 1:1. The coupling efficiency is 95%. The laser crystal is a 1.0 at. % $Nd^{3+}$ doped, Φ4 mm × 3 mm Nd:YAG wrapped with indium foil, and mounted at a TEC (thermal electronic cooled) copper block, and the temperature is maintained at 20 °C. The whole cavity is also cooled by TEC. Both sides of the laser crystal were coated for high

a)Electronic mail: optik@sina.com

 

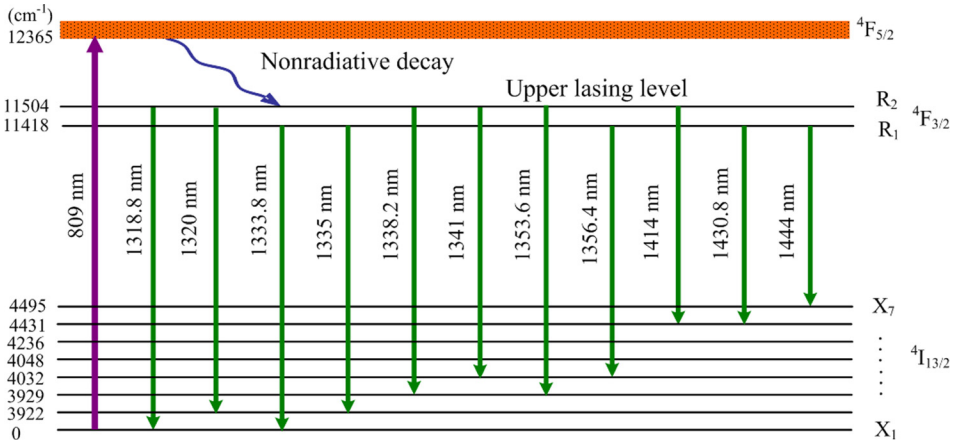


FIG. 1. Energy structure of a Nd:YAG crystal based on the $^4F_{3/2}$–$^4I_{13/2}$ transition.

transmission (HT) from 1330 to 1340 nm. The Brewster angle (BP) was used in order to achieve polarized beam. The plane mirror (M1) of the cavity is HT at the pump wavelength and highly reflective (HR) from 1330 to 1340 nm. The concave mirror (M2) is an output coupler, which was coated with a transmission of 2.8% from 1330 to 1340 nm. A KDP crystal lens (RoC = −200 mm) is inserted in the cavity. Both end facets of the KDP crystal lens are AR coated from 1330 to 1340 nm to reduce the reflection losses in the cavity. The optical axis ($c$-axis) and $b$-axis of the KDP crystal are, respectively, perpendicular and horizontal to the optical axis of the resonator, and the $a$-axis is also perpendicular to the optical axis of the resonator (see Fig. 2). The beam in the cavity is horizontally polarized. The horizontally polarized light is divided into the ordinary ray and the extraordinary ray in the crystal. The difference between the refractive indices of the ordinary ray and the extraordinary ray makes the KDP crystal act as a birefringent filter. Combined with the BP, the KDP crystal lens formed a Lyot filter and compressed the available gain bandwidth.

Equation (1) is the round transmittance $T_\lambda$ of the Lyot filter

$$T_\lambda = \cos^2\left[4\pi(n_x - n_e)d/\lambda\right], \tag{1}$$

where $n_x = n_o - 1/2n_o^3\gamma_{63}E$ is the refractive index of the ordinary ray when applying the electric field to the KDP crystal lens, $n_o$ is the refractive index of the ordinary ray, $\gamma_{63}$ is the electrooptic coefficient, $E = U/D$ is the electric field intensity, $U$ is the voltage, $D$ is the distance between the two electrodes, $n_e$ is the refractive index of the extraordinary ray ($n_e$ is constant when applying voltage in the direction of the $c$-axis of the KDP crystal lens), $d$ is the center thickness of the KDP crystal lens, and $\lambda$ is the laser wavelength. The refractive indices of the ordinary ray and the extraordinary ray are, respectively, 1.5115 and 1.4698. According to Eq. (1), $T_{1333.8\,\mathrm{nm}} = 100\%$, $T_{1335\,\mathrm{nm}} = 2.32\%$, and $T_{1338.2\,\mathrm{nm}} = 1.40\%$ when applying the voltage of 0.69 kV. Namely, the oscillation of 1333.8 nm is achieved by suppressing the oscillation of 1335 nm and 1338.2 nm. By adjusting voltage to 3.5 kV, $T_{1335\,\mathrm{nm}} = 100\%$, $T_{1333.8\,\mathrm{nm}} = 2.77\%$, $T_{1338.2\,\mathrm{nm}} = 3.26\%$. Therefore, the oscillation of 1335 nm is achieved. Similarly, the oscillation of 1338.2 nm is achieved by adjusting voltage.

Because of certain fundamental physics mechanisms, e.g., the quantum defect and fluorescence quenching, it is inevitable that a larger amount of absorbed energy transfers into the heat in the laser rod, which produces an uneven temperature field and greatly reduces the beam quality.[19] Therefore, it has been a long-term active subject to study the heat generation mechanism and its interaction with other physics mechanisms in solid-state lasers.[20,21] To compensate for the thermal lens effect of the laser rod, we shaped the KDP crystal into concave lens (see Fig. 2). As KDP crystal lens has electro-optical characteristics, we can change its refractive index by applying voltage perpendicularly to the optical axis, which can change the focal length of the lens. Hence, by adjusting the focal length of the KDP crystal lens, we could compose a Galileo telescope system consisting of the thermal lens of the laser rod and KDP crystal lens. Thus, the thermal lens effect can be well compensated. Several methods are used to compensate for the thermal lens effect. The first is using the thermal-insensitive resonator.[22] The

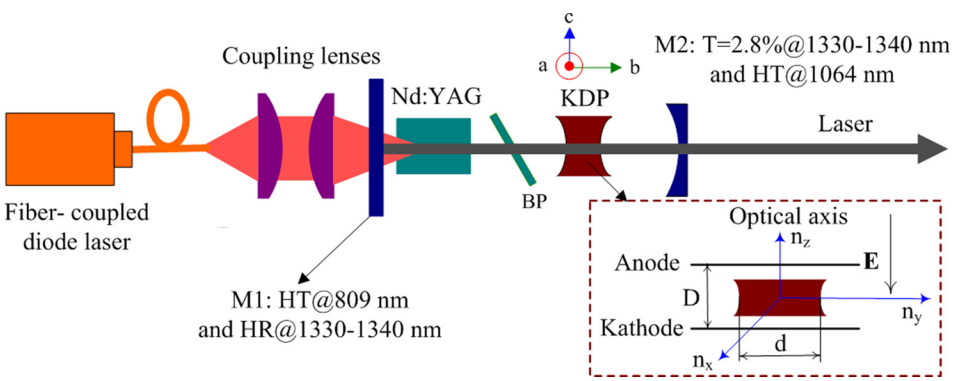


FIG. 2. Experimental configuration of the fine wavelength control in 1.3 $\mu$m Nd:YAG lasers.

second is manufacturing the end of the laser rod into a concave shape, which could act as the role of a negative lens compensation for the thermal lens effect.[23] The third is inserting a negative focus device in the cavity.[24] However, the first method can be used only in the case of a long focal length of the thermal lens (<50 mm). The other two methods could only show good performance under certain pump power. In addition, to improve the mechanical arrangement (deformable mirrors,[25] moveable lens,[26] and resonator length adjustments[27]), Graf *et al*. and Wyss *et al*. proposed using an adaptive negative lens to compensate for the power-dependent thermal lens.[28,29] This method could generate a strong negative lens to effectively compensate for the thermal effect; however, it is difficult to manufacture the compensating disk. The method we raised could compensate for the thermal lens effect in a wide range of thermal focal length change, and the KDP crystal is very easy to manufacture.

Figure 3 presents the dependence of the output power on the incident pump power for the Nd:YAG laser at 1333.8 nm. In a frame in the top left corner of Fig. 3, a scaled plot of a part of the spectrum is shown. It can be seen that oscillation of 1335 nm was suppressed by the Lyot filter, and only the 1333.8 nm output was realized. The output power reaches 1.03 W at an incident pump power of 18.4 W. The corresponding optical-to-optical conversion efficiency is 5.6% with a slope efficiency of approximately 6.5%. With this configuration, we recorded an oscillation threshold at 2.4 W. Some intensity stability testing was carried out by monitoring the 1333.8 emission with a Field-Master-GS powermeter at 10 Hz. The fluctuation of the output power is about 2.3% in 4 h. The short-term power stability is measured by a LabMaster Ultima that operates at 50 kHz, and the percent rms noise value is 2.8%. The thermal stability of the output wavelength was also observed at different pump powers. We found that the change range of central wavelength maintains less than ±0.01 over the full range of pump powers. The optical spectrum was measured with a Spectrapro-500i spectrometer from Acton Research Corporation (see Fig. 3 inset). The spectral linewidth (FWHM definition) is about 0.25 nm with the central wavelength at 1338.2 nm. The $M^2$ factor is about 1.05 measured by knife-edge technique. The output power at 1335 nm versus the incident pump power is shown in Fig. 4. In a frame in the top left corner of Fig. 4, a scaled plot of a part of the spectrum is shown. The spectral linewidth is about 0.3 nm with the central wavelength at 1335 nm. The output power of 1335 nm was 1.36 W and the optical-to-optical efficiency was 7.4%. The slope efficiency with respect to the incident pump power was 8.2%. The threshold pump power is 1.9 W. The $M^2$ factor is about 1.12. The long-term intensity stability of the laser is better than 1.8%. The laser performance of 1338.2 nm is presented in Fig. 5. The measured optical spectrum at the maximum output power is depicted in the inset of Fig. 5. The output power was 4.59 W and the optical-to-optical efficiency was 24.9%. The slope efficiency and the threshold were 26.9% and 1.3 W, respectively. The $M^2$ factor and the long-term stability were 1.06 and 1.4%, respectively.

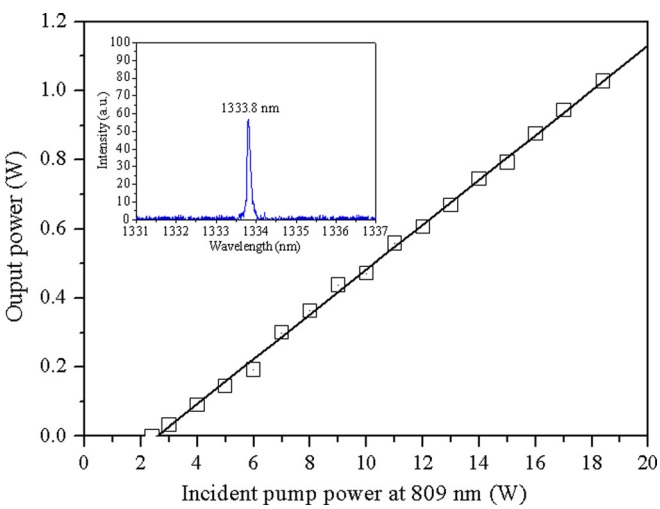


FIG. 3. Output power versus the incident pump power for the 1333.8 nm emission. Inset: optical spectrum of the 1333.8 nm emission at the maximum output power.

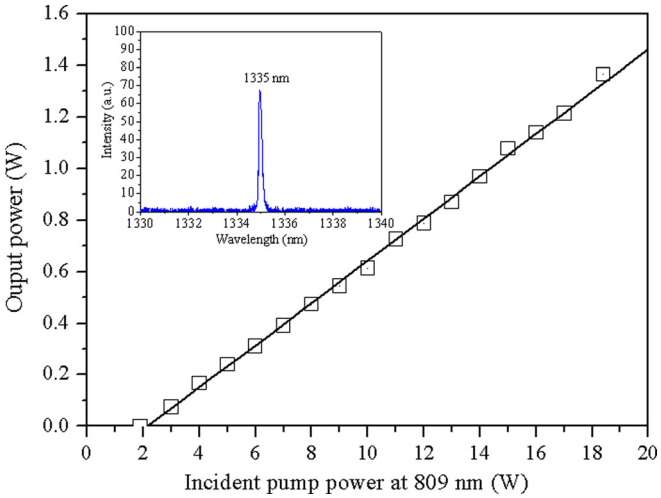


FIG. 4. Output power versus the incident pump power for the 1335 nm emission. Inset: optical spectrum of the 1335 nm emission at the maximum output power.

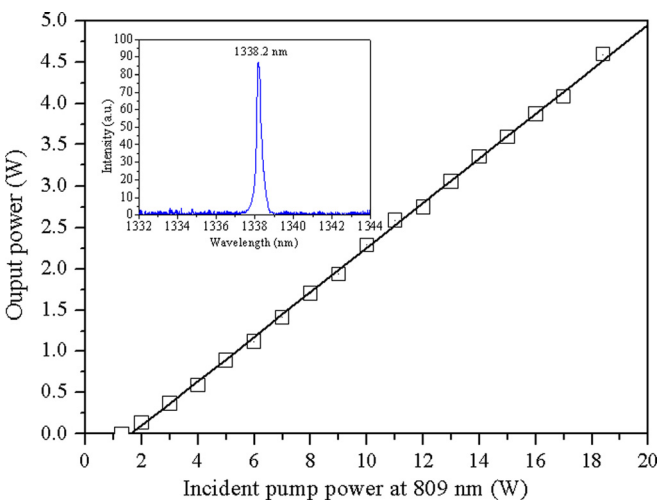


FIG. 5. Output power versus the incident pump power for the 1338.2 nm emission. Inset: optical spectrum of the 1338.2 nm emission at the maximum output power.

Equation (2) is the free spectral range $\Delta\lambda_F$ of the KDP electro-optical crystal lens

$$\Delta\lambda_F = \lambda^2/2(n_x - n_e)d. \quad (2)$$

To achieve the multi-wavelength operation, we increase the free spectral range by changing the length of KDP crystal. When the center thickness of KDP crystal was 4 mm and the adjusting voltage was 1.2 kV, according to Eqs. (1) and (2), $\Delta\lambda_F \approx 5$ nm, $T_{1333.8\,\mathrm{nm}} = 100\%$, $T_{1335\,\mathrm{nm}} = 92.4\%$, $T_{1338.2\,\mathrm{nm}} = 1.19\%$. Thus, according to the condition of multi-wavelength oscillation,[30] a dual-wavelength emission at 1333.8 and 1335 nm was achieved. Figure 5 shows the output power at each lasing wavelength with respect to the incident pump power at 809 nm. The threshold of pump power is 2.5 W for 1333.8 nm, and 2.2 W for 1335 nm. The output power of 1335 nm line increases monotonically as the pump power increases. On the other hand, the output power of 1333.8 nm line first increases linearly with the pump power, reaches its maximum power of 0.47 W at the pump power of 14.1 W, and then descends monotonically. We believe that the gain competition between 1335 nm and 1333.8 nm lines leads to the output power of 1333.8 nm decreases over 14.1 W of pump power. The laser beams were observed at different pump powers. The $M^2$ factor of 1333.8 nm emission is estimated to be approximately 1.14 near threshold, and then increases to 2.45 at pump power greater than 18.4 W. On the other hand, the 1335 nm emission maintains the beam quality factor $M^2$ less than 1.13 over the full range of pump powers. The long-term intensity stability for 1333.8 nm and 1335 nm emissions at the pump power of 18.4 W is about 5.2% and 2.1%, respectively. The inset of Fig. 6 shows the measured optical spectrum for the dual-wavelength laser at the pump power of 18.4 W. The central wavelengths are 1333.8 nm and 1335 nm, with the spectral linewidths of 0.25 nm and 0.32 nm, respectively. Similarly, a triple-wavelength emission at 1333.8, 1335, and 1338.2 nm was achieved by adjusting voltage to 0.6 kV. The output powers at each lasing wavelength versus incident power are given in Fig. 7. It can be seen the output power of 1338.2 nm increases quadratically as the incident pump power

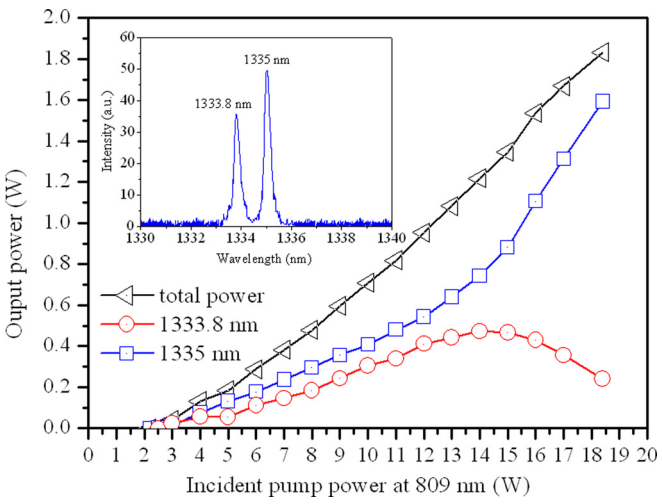


FIG. 6. Output powers versus the incident pump power for dual-wavelength operation. Inset: optical spectrum of dual-wavelength operation.

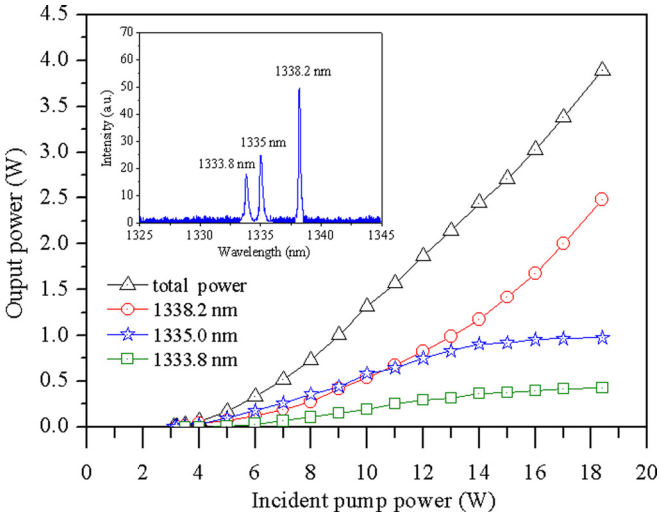


FIG. 7. Output powers versus the incident pump power for triple-wavelength operation. Inset: optical spectrum of triple-wavelength operation.

increases. And the output power of 1335 nm rises monotonically with the incident pump power. On the other hand, as the incident pump power was increased, the 1333.8 nm transitions was not suppressed completely by the 1335 nm and 1338.2 nm transitions, but the three wavelengths competed with each other. The output power proportion of 1333.8 nm, 1335 nm, and 1338.2 nm was 1:2.3:5.8. A total output power of 3.89 W for the triple-wavelength was achieved at the incident pump power of 18.4 W with optical conversion efficiency of 13.6%. The measured optical spectrum for the triple-wavelength laser at the maximum output power is depicted in the inset of Fig. 7. The long-term intensity stability of 1333.8 nm, 1335 nm, and 1338.2 nm emissions at the maximum output power are about 4.2%, 5.6%, and 3.3%, respectively.

## III. CONCLUSION

In conclusion, we have demonstrated an all-solid-state tunable Nd:YAG laser based on the $^4F_{3/2}-{}^4I_{13/2}$ transition with an electro-optical crystal lens. With an adjustable voltage applied to the KDP crystal lens, the laser wavelength could be tuned from 1333.8 to 1338.2 nm. By adjusting the free spectral range of the Lyot filter, a dual-wavelength Nd:YAG laser at 1333.8 nm and 1335 nm has also been demonstrated. At an incident pump power of 18.4 W, the output power obtained at 1333.8 nm and 1335 nm is 0.24 W and 1.59 W, respectively. And a cw emission of triple-wavelength 1333.8, 1335, and 1338.2 nm has been achieved. A total output power of 3.89 W was yielded with optical conversion efficiency of 13.6%. Thus, this wok presents a new method to realize tunable and multi-wavelength solid-state laser. The method avoids mechanical modulation, so it is simpler, more precise, and applicable, which can also be popularized in other solid-state lasers.

## ACKNOWLEDGMENTS

This work was supported by the National Natural Science Foundation of China (Grant Nos. 61108029 and 61275135).

[1]G. Zhang, H. Shen, R. Zeng, C. Huang, W. Lin, and J. Huang, Opt. Commun. **183**, 461 (2000).
[2]Z. Sun, R. Li, Y. Bi, X. Yang, Y. Bo, W. Hou, X. Lin, H. Zhang, D. Cui, and Z. Xu, Opt. Express **12**, 6428 (2004).
[3]S. Singh, R. G. Smith, and L. G. Van Vitert, Phys. Rev. B **10**, 2566–2572 (1974).
[4]F. Balembois, M. Castaing, E. Hérault, and P. Georges, Laser Photon. Rev. **5**(5), 659–676 (2011).
[5]M. Castaing, E. Hérault, F. Balembois, P. Georges, C. Varona, and P. Loiseau, Opt. Lett. **32**, 799 (2007).
[6]Q. Wang, Z. Wei, Y. Zhang, Z. Zhang, H. Yu, H. Zhang, and Z. Wang, Opt. Lett. **36**(10), 1770 (2011).
[7]W. Shi, Y. J. Ding, N. Fernelius, and K. Vodopyanov, Opt. Lett. **27**, 1454–1456 (2002).
[8]J. F. Federici, B. Schulkin, F. Huang, D. Gary, R. Barat, F. Oliveira, and D. Zimdars, Semicond. Sci. Technol. **20**, S266 (2005).
[9]J. B. Baxter and G. W. Guglietta, Anal. Chem. **83**, 4342 (2011).
[10]C. B. Reid, E. Pickwell-MacPherson, J. G. Laufer, A. P. Gibson, J. C. Hebden, and V. P. Wallace, Phys. Med. Biol. **55**, 4825 (2010).
[11]H. Y. Zhu, G. Zhang, C. H. Huang, Y. Wei, L. X. Huang, A. H. Li, and Z. Q. Chen, Appl. Phys. B **90**, 451 (2008).
[12]R. Zhou, B. G. Zhang, X. Ding, Z. Q. Cai, W. Q. Wen, P. Wang, and J. Q. Yao, Opt. Express **13**, 5818 (2005).
[13]Y. F. Chen, M. L. Ku, and K. W. Su, Opt. Lett. **30**, 2107 (2005).
[14]C. Ren and S. L. Zhang, J. Phys. D: Appl. Phys. **42**, 155107 (2009).
[15]B. Wu, P. P. Jiang, D. Z. Yang, T. Chen, J. Kong, and Y. H. Shen, Opt. Express **17**, 6004 (2009).
[16]Y. P. Huang, C. Y. Cho, Y. J. Huang, and Y. F. Chen, Opt. Express **20**, 5644 (2012).
[17]V. E. Nadtocheev and O. E. Nanii, Sov. J. Quantum Electron. **19**, 444 (1989).
[18]R. Zhou, W. Wen, Z. Cai, X. Ding, P. Wang, and J. Yao, Chin. Opt. Lett. **3**(10), 597–599 (2005), available at http://www.opticsinfobase.org/col/abstract.cfm?uri=col-3-10-597.
[19]J. D. Foster and L. M. Osterink, J. Appl. Phys. **41**, 3656 (1970).
[20]F. Song, C. Zhang, X. Ding, J. Xu, and G. Zhang, Appl. Phys. Lett. **81**, 2145 (2002).
[21]S. R. Bowman, S. P. O'Connor, and S. Biswal, IEEE J. Quantum Electron. **41**, 1510 (2005).
[22]J. Steffen, J. P. Lortscher, and G. Herziger, IEEE J. Quantum Electron. **8**, 239 (1972).
[23]S. Lee, M. Yun, B. H. Cha, C. J. Kim, S. Suk, and H. S. Kim, Appl. Opt. **41**, 5625 (2002).
[24]J. Sherman, Appl. Opt. **37**, 7789 (1998).
[25]U. J. Greiner and H. H. Klingenberg, Opt. Lett. **19**, 1207 (1994).
[26]S. Jackel, I. Moshe, and R. Lavi, Proc. SPIE **3611**, 42 (1999).
[27]D. C. Hanna, C. G. Sawyers, and M. A. Yuratich, Opt. Quantum Electron. **13**, 493 (1981).
[28]T. Graf, E. Wyss, M. Roth, and H. P. Weber, Opt. Commun. **190**, 327 (2001).
[29]E. Wyss, M. Roth, T. Graf, and H. P. Weber, IEEE J. Quantum Electron. **38**, 1620 (2002).
[30]H. Y. Shen, R. R. Zeng, and Y. P. Zhou, Appl. Phys. Lett. **56**, 1937 (1990).